



## **Comparison of Softening Behavior and Abrasive Wear Resistance between Conventionally and Additively Manufactured Tool Steels**

Downloaded from: <https://research.chalmers.se>, 2025-12-04 23:23 UTC

Citation for the original published paper (version of record):

Yuan, M., Nyborg, L., Oikonomou, C. et al (2024). Comparison of Softening Behavior and Abrasive Wear Resistance between Conventionally and Additively Manufactured Tool Steels. Steel Research International, 95(6).  
<http://dx.doi.org/10.1002/srin.202300577>

N.B. When citing this work, cite the original published paper.

# Comparison of Softening Behavior and Abrasive Wear Resistance between Conventionally and Additively Manufactured Tool Steels

Miwen Yuan, Lars Nyborg, Christos Oikonomou, Yicheng Fan, Libin Liu, Jason Weijiang Ye, and Yu Cao\*

Directed energy deposition (DED) is a powerful method for hard-facing the existing tool components. Herein, three tool steel grades including a newly developed maraging steel (NMS), a cold work tool steel (V4E), and a high boron steel (HBS) are cladded on a hot work tool steel substrate. After tempering, the cladded tool steels are exposed to high temperatures at 600, 700, and 800 °C for 3 h to evaluate their softening resistance. The results show that all three tool steel grades have a significant hardness drop when the softening temperature reaches 700 °C. The investigated NMS has the lowest initial hardness in the tempered state but the best softening resistance. In contrast, HBS has the highest initial hardness but the worst softening resistance among the three steel grades. V4E tool steel has a moderate softening resistance compared to the other two steel grades. The factors contributing to the softening resistance have been discussed. Corresponding conventional tool steels are also adapted as references for comparison. Except for the NMS, the additive manufacturing tool steel samples have a better softening resistance than the conventional counterparts owing to more alloying elements trapped in the matrix. The abrasive wear resistance of the tempered and softened tool steels manufactured by DED and conventional methods is also evaluated and the wear mechanism is discussed. Besides the hardness, the free spacing  $\lambda$  between coarse hard particles is one of the major factors influencing the abrasive wear resistance.

combination of wear resistance and softening resistance is necessary for tool steels. How to improve the duration of hot stamping dies is a widely discussed topic, especially for large dies made of the expensive hot-working tool steel considering the cost. In addition, the dies entirely made by high-alloy tool steels sometimes cannot meet certain requirements, such as thermal fatigue resistance and toughness. One way to extend the lifetime of the tools is thin layer deposition techniques (e.g., physical vapor deposition (PVD), chemical vapor deposition (CVD)) which can provide protective layers on the die surface and significantly improve the surface hardness and wear resistance. Beake et al.<sup>[2]</sup> conducted a PVD coating of AlCrN-TiAlN bilayer on H13 tool steel and found that the tool life of the coated tools could be improved by  $\approx 100\%$  compared to the single TiAlN layer. Pellizzari<sup>[3]</sup> found that the duplex-PVD coating sample shows an outstanding wear behavior than the nitride one against 6082 Al alloy in high load. High surface hardness with good stability against chemical dissolution was considered as the reason.

## 1. Introduction

Tool steels are widely applied to make molds, die, and other components that require high wear resistance.<sup>[1]</sup> In hot stamping, a

However, due to the incompatibility between the layers and the substrate, the coatings could be worn out and peeled off after being subjected to a long term of wear, cyclic heating, and cooling during the hot stamping process. In general, PVD and CVD


M. Yuan, L. Nyborg, Y. Cao  
Department of Industrial and Materials Science  
Chalmers University of Technology  
41296 Gothenburg, Sweden  
E-mail: yu.cao@chalmers.se

M. Yuan, L. Liu  
School of Materials Science and Engineering  
Central South University  
Changsha 410083, P. R. China

C. Oikonomou  
Research and Development Department  
Uddeholms AB  
63885 Hagfors, Sweden

Y. Fan  
Laser Cladding Department  
ASSAB Tooling Technology (Shanghai) Co., Ltd  
Shanghai 201108, P. R. China

J. W. Ye  
Voestalpine High Performance Metals Pacific Pte Ltd  
Singapore 048424, Singapore

 The ORCID identification number(s) for the author(s) of this article can be found under <https://doi.org/10.1002/srin.202300577>.

© 2024 The Authors. Steel Research International published by Wiley-VCH GmbH. This is an open access article under the terms of the Creative Commons Attribution-NonCommercial-NoDerivs License, which permits use and distribution in any medium, provided the original work is properly cited, the use is non-commercial and no modifications or adaptations are made.

DOI: 10.1002/srin.202300577

layers have a comparatively lower load-bearing capability. Once the coating layers get damaged, it is hard to restore their performance through polishing. In this case, thermochemical coatings (e.g., boriding, nitriding) could be an alternative way.<sup>[4]</sup> Nitrogen or boron atoms diffuse into steels at high temperatures and from ceramic compound phase. The surface of the steels will then be harder and have a high wear resistance. However, the treated surface may be sensitive to thermal fatigue and have a relatively high friction with counterparts.<sup>[3]</sup> Therefore, from the perspective of economy and duration of the dies, we are chasing a method to enhance the wear resistance of hot working die in a cost-effective and flexible way.

Laser directed energy deposition (DED), one of the additive manufacturing (AM) technologies, is a good option for cladding new materials on the die surface. Both powder and wire can be used as feedstock. Considering the cost of manufacturing, Wire arc additive manufacturing (WAAM) has the capability to rapidly produce large components and is considered the most cost-effective option among the DED technologies because it can use existing arc-welding robots and power supplies.<sup>[5]</sup> The building rate of WAAM is in the range of 1–10 kg h<sup>-1</sup>,<sup>[6]</sup> which is much faster than the laser-powder DED technology. However, the disadvantages of WAAM are low accuracy, limited material options, and rough surface finish. Therefore, laser powder DED is more common.

In the tooling industry, laser powder DED can be used not only to modify the surface properties of the dies for hot stamping but also to repair the dies. So far, laser cladding of tool steels has been extensively studied. Kattire et al.<sup>[7]</sup> cladded a cold work tool steel grade (CPM 9 V) on H13 steel for repair applications. The results showed that the clad quality was sensitive to the processing parameters. Leunda et al.<sup>[8]</sup> deposited CPM 10 V and Vanadis 4 Extra cold work tool steel grades on the Vanadis 4 Extra substrate and found that the cladded zone is crack-free. However, the high strength and low toughness of tool steels make cracking one of the main problems that prevent the application of AM tool steels.<sup>[9]</sup> In addition, whether the properties of the cladded steels are comparable to the conventional counterpart is uncertain. Because the microstructure of the materials fabricated by the laser cladding technique could be significantly different from the conventional counterparts, the material properties, such as softening resistance and wear behaviors, could hence be different.

For hot stamping, the wear resistance of the cladded materials is of great importance. Wang et al.<sup>[1]</sup> found that the fraction, morphology, and distribution of the hard phases can distinctly influence the abrasive wear resistance of laser-cladded tool steels. Large carbides are beneficial for abrasive wear resistance, while tiny carbides can be scratched away easily. On the contrary, the research by Orečný et al.<sup>[10]</sup> shows that the tool steel with fine carbides dispersed in the matrix has higher wear resistance. The influence of carbides/strengthening phases on wear resistance is of interest for further studies. From the two reports by Colaço et al.<sup>[11,12]</sup> the laser-cladded martensitic tool steels (AISI 420 and X42Cr13) showed higher wear resistance compared with the conventional quenched and tempered samples with similar hardness. Rahman et al.<sup>[13]</sup> investigated a laser-cladded high-speed steel and found that the cladded steel has a superior wear resistance to the conventional one. Still, there are few reports on the comparison of wear properties between laser cladding tool steels and conventional ones.

Since stamping dies are subject to high temperatures and high loads, the deposited material is required to have high hardness, high abrasive-adhesive wear resistance, and good temper-back resistance. In the present study, several grades of tool steels were cladded on Uddeholm Dievar hot work tool steel (modified from H13) by means of DED for the hard-facing purposes. The softening resistance of the cladded tool steels subjected to high-temperature exposure was evaluated. The abrasive wear resistance of the samples before and after being softened was also investigated. As a comparison, their corresponding conventional tool steels were heat-treated and tested under the same procedure as being done on the cladded counterparts. Through this study, the influence of strengthening phases in tool steels on softening resistance and abrasive wear resistance is expected to be better understood.

## 2. Experimental Section

In the present study, three types of tool steels, a high-boron steel grade (HBS, X50MoCoCr17-4), Uddeholm Vanadis 4 Extra (V4E), and a newly developed maraging steel (NMS), were cladded on the base material plate with the size of 127 × 58 × 25 mm. The composition of the base steel and the cladded tool steels are given in **Table 1**. The materials were supplied by Uddeholm AB. The processing parameters of DED can be found in a previously published article.<sup>[14]</sup> After cladding, tempering was performed. Notice that DED is a relatively new fabrication method for these materials. Considering hardness is one of the most important factors that determine the wear resistance, the tempering parameters were optimized to yield the highest hardness value in the early stage of the project. A series of tempering parameters including temperatures and time (525, 535, and 550 °C, for 2 h-2times, 2 h-3times, and 3 h-2times) were examined. The details were not provided due to the length limit of the article. The optimized parameters for heat treatment are given in **Table 2**. For comparison, conventional counterparts (Con.), i.e., hot isostatic pressed (HIP) HBS and NMS, as well as forged V4E, were hardened and tempered using well-established parameters in the industry practice, as listed in Table 2. To examine softening resistance, heat treatments were conducted on both conventional and DED-processed (AM) samples at elevated temperatures of 600, 700, and 800 °C for 3 h.

Cylinder samples with 12 mm in diameter and 20 mm in height were used for the abrasive wear test using a steel wheel abrasive test instrument modified from a grinding machine. Both as-tempered and softened samples were measured. Before the test, the top surface was machined into a flat plane by using an industrial planar grinding machine. In the abrasive wear test, the steel samples were under a normal load of 17.8 N against an aluminum oxide sandpaper with a particle size of P 800. The

**Table 1.** The chemical composition of the studied steels, in wt%.

	C	Si	Mn	Cr	Mo	Co	V	Ni	Cu	Fe
V4E	1.4	0.40	0.40	4.7	3.5	–	3.7	–	–	Bal.
NMS	0.03	0.35	0.40	5.0	8.0	12.0	–	2.0	2.0	Bal.
Base material	0.38	0.30	0.75	2.6	2.25	–	0.9	–	–	Bal.

**Table 2.** Heat treatment parameters used for the steels in this investigation.

	Manufacturing method	Heat treatment performed
HBS	DED	525 °C – 2 h × 2 times
	HIP	1100 °C for 1 h in vacuum T8/5 <sup>a)</sup> 100 s; 525 °C 1 h × 3 times
V4E	DED	550 °C – 2 h × 3 times
	HIP and forged	1150 °C for 10 min T8/5 <sup>a)</sup> 300 s; 525 °C 1 h × 3 times
NMS	DED	535 °C – 3 h × 2 times
	HIP	

<sup>a)</sup>T8/5: Cooling time from 800 to 500 °C.

sandpaper was renewed every 15 s and the total testing time for each sample was 60 s. During the test, the sandpaper was wetted by a water flow of 1.5 L min<sup>-1</sup>. After the test, the weight reductions of dry samples were recorded by an electronic balance. Wear resistance was assessed by the weight reduction in mg min<sup>-1</sup>. Notice this method cannot fully simulate the conditions of the hot stamping process which includes both abrasive and adhesive wear against work material in the absence of water. The test results in this article only provide the basic knowledge of abrasive wear resistance of tool steel at room temperature.

The microstructure and the topography of worn surfaces were characterized by scanning electronic microscopy (SEM) using LEO/ZEISS Gemini 1550. To analyze the strengthening phases in the tool steels, microstructures of the polished and etched samples were imaged by SEM in the secondary electron (SE) mode. ImageJ software was applied to statistically analyze the SEM images. The chemical compositions of the phases in steel samples were analyzed by using a PHI 700 scanning Auger electron spectroscopy (AES). The accelerating voltage and the current of the electron beam were 10 kV and 10 nA, respectively. Hardness was measured by a DuraScan 70-G5 instrument. The testing load is 10 kg, and the dwell time is 15 s. Six indentations were performed on each sample to obtain the average hardness.

### 3. Results

#### 3.1. Microstructure Evolution of the Tool Steels during Softening

Figure 1 shows the microstructure evolution in both HIP-processed and DED-fabricated HBS steels during softening. In the as-tempered condition, nearly spherical bright particles were dispersed in the HIP-fabricated HBS steel (Figure 1a). These particles should be primary borides and were confirmed as M<sub>3</sub>B<sub>2</sub> by X-Ray diffraction (XRD) in Figure 2a. Besides body-centered cubic (bcc) phase and primary boride, no other phase was found in the matrix. After being softened at 600 °C, no precipitate was observed in the matrix (Figure 1b). However, when the softening temperature was increased to 700 °C, some fine precipitates were found in the matrix of the steel (Figure 1c). These precipitates were coarsened at 800 °C (Figure 1d). According to the XRD results (Figure 2a), these precipitates should be M<sub>23</sub>C<sub>6</sub> and M<sub>6</sub>C carbides. To further confirm it, AES was applied to analyze the composition of the phases. As shown in Figure 3, a high concentration of B, Mo was confirmed in the square shape boride. The matrix of course has strong Fe peaks. For the white precipitates (location 3), the spectra clearly showed C and Mo peaks. The peak of B has not been revealed, which means the white precipitates should be carbides enriched with Mo. They are probably the M<sub>6</sub>C type.

It should be noticed that some microcracks were found in some big borides in the samples softened at 700 and 800 °C (Figure 1c,d), as marked by the white arrows. These microcracks were formed during the cooling from the softening temperatures and were probably caused by the stresses induced by different thermal expansion coefficients between the matrix and the boride phase. From the calculation by JmatPro, the unit volume change of the M<sub>3</sub>B<sub>2</sub> phase is from 1.000 (25 °C) to 1.026 (800 °C), while for ferrite phase, it is from 1.000 (25 °C) to 1.037 (800 °C). It means that when the material was cooled down to room temperature, the matrix (ferrite phase) would have a more distinct contraction, leading to compressive stress on the ceramic boride particles. Consequently, the brittle boride particles could be broken. With the increase in softening temperature, the number of

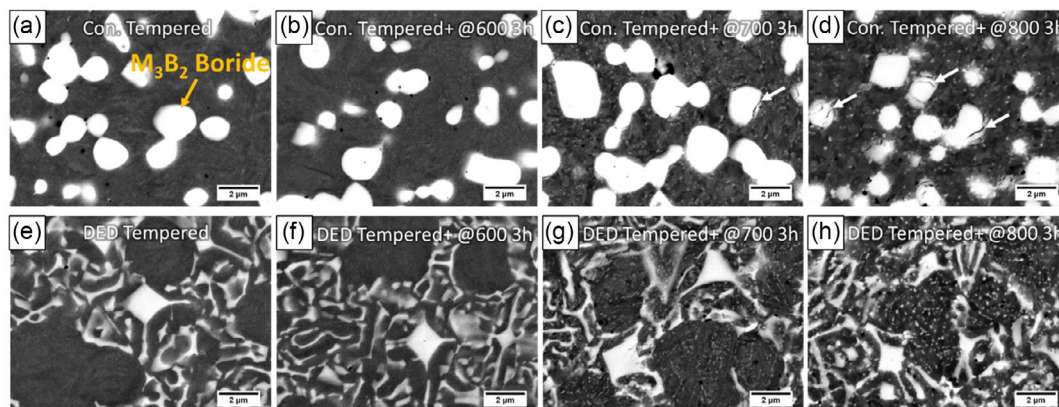


**Figure 1.** a–d) BSE images of HIP-processed and e–h) DED-processed HBS after being softened at different temperatures for 3 h: a,e) as tempered without softening, b,f) 600 °C, c,g) 700 °C, and d,h) 800 °C.



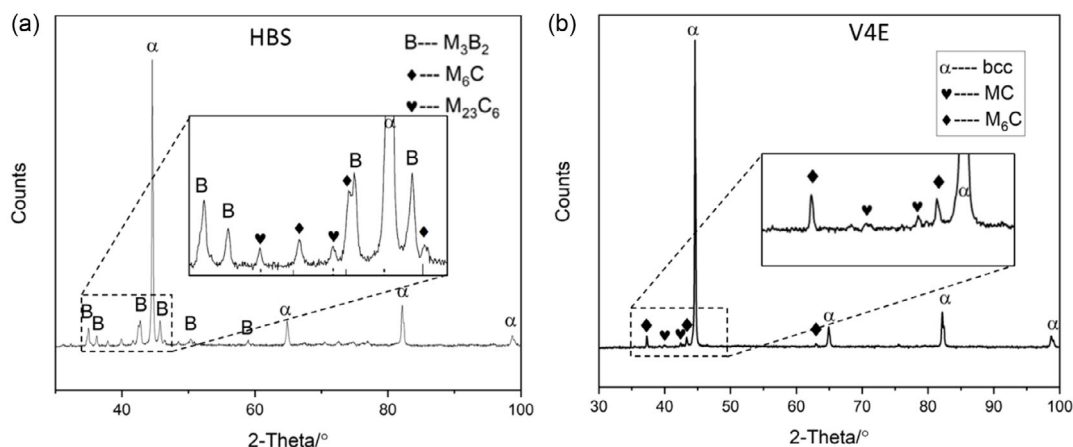


**Figure 2.** XRD patterns of the softened steels at 800 °C for 3 h: a) DED-fabricated HBS, and b) HIP-fabricated V4E steel.

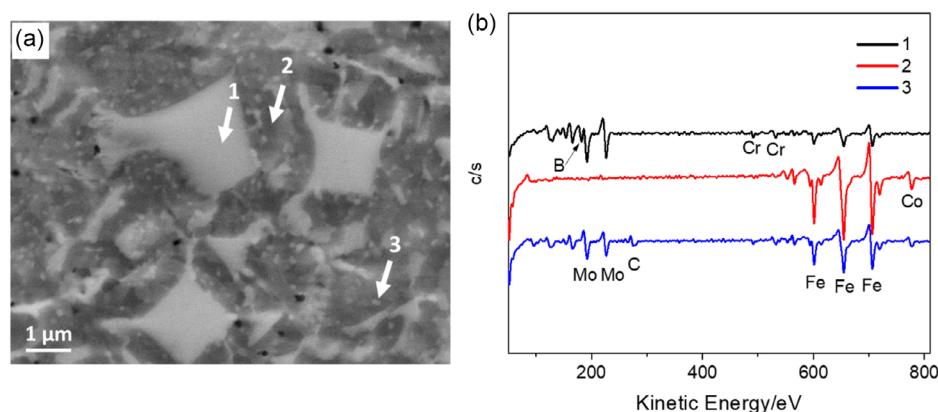


**Figure 3.** AES analysis conducted on HBS after being softened at 800 °C for 3 h: a) SEM image providing analysis locations, b) AES spectra. Position 1 (boride) shows the peaks of B and Mo. Position 2 (base material) shows a strong peak of Fe. Position 3 (precipitates) shows enrichments of Mo, C, and Fe.

microcracks tended to increase. This can be explained by larger thermal contraction when cooling from higher temperatures.

Regarding the proportion of the bright borides in the materials, no significant change was detected at different softening temperatures, as confirmed by the statistical analysis using ImageJ in **Figure 4**. The area percentage of these bright borides was maintained at a level of  $\approx 21\%$  under all conditions. Moreover, the size of these borides was kept between 1.2 and 1.3  $\mu\text{m}$  and did not change significantly with temperature either, as shown in **Figure 4**.

For the DED-fabricated HBS steel, as shown in **Figure 1e**, the boride particles were presented in two morphologies: one had a square shape, and another was in the form of a eutectic structure. The boride particles in the DED-fabricated sample had a much smaller average size ( $\approx 0.4 \mu\text{m}$ ) compared to that of the HIP-fabricated samples ( $\approx 1.2\text{--}1.3 \mu\text{m}$ ). In addition, there existed particle-free areas. With the increase in softening temperatures, fine precipitates became visible in the matrix after heating at 700 °C (**Figure 1g**) and coarsened at 800 °C (**Figure 1h**). In addition, it

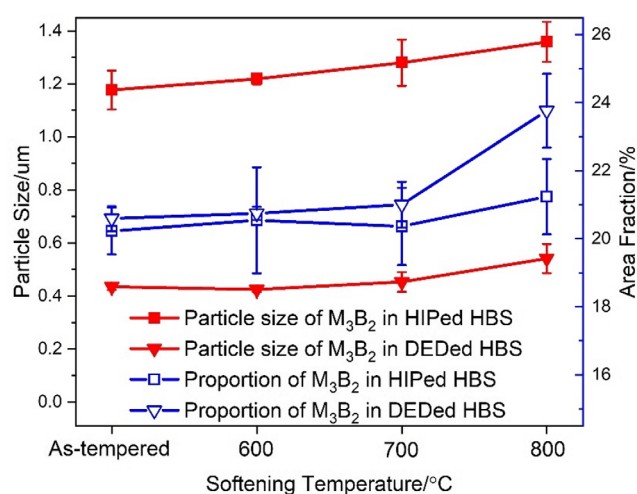


**Figure 4.** The evolution of the average size and area fraction of the borides after the softening at 600–800 °C for HBS.

seemed that there were more precipitates in the DED-fabricated sample than in the HIP-fabricated one after softening at 800 °C. The possible reason could be that more alloying elements were trapped in the matrix due to the fast solidification in DED-fabricated samples, leading to an increased fraction of precipitates. Anyway, the DED and HIP-fabricated variants of HBS showed similar precipitation behavior during the softening process (Figure 1).

**Figure 5** shows the microstructure evolution of conventional and DED-fabricated V4E steel during the softening treatments. The microstructural change in the conventional and DED-fabricated V4E is similar to that in HBS. A noticeable phenomenon was that the major primary particles in V4E were dark in backscattered electron (BSE) images. These dark primary particles were confirmed as MC-type (M refers to metal elements, and C refers to Carbon) carbide enriched with V in the previous studies.<sup>[14,15]</sup> Energy-dispersive X-Ray spectroscopy (EDS) mapping analysis was also performed on the tempered conventional V4E sample. As shown in **Figure 6**, the dark particles are mainly enriched with V element and partly enriched with Mo. Vanadium and carbon have a relatively lower average atomic number compared to Fe, making MC carbides present a dark illumination in the BSE imaging mode. The average size of MC particles was about 0.5  $\mu\text{m}$  in conventional samples (Figure 5a–d). For DED-fabricated V4E samples, primary MC carbide had a varied morphology and was presented in the form of a eutectic structure (Figure 5e–h). The average MC particle size was 0.2  $\mu\text{m}$ , which was smaller than that of the conventional counterparts ( $\approx 0.5 \mu\text{m}$ ). In **Figure 7**, it also can be seen that the fraction and size of primary MC carbide in both conventional and AM-produced V4E steel are rather stable during the softening process. The proportion of MC primary carbide (the coarse type) in AM V4E (5.5%) was lower than that in forged ones (7.1%).

When the softening temperature was increased to 700 °C, some tiny bright precipitates were found in the matrix of conventional V4E (Figure 5c). These precipitates were suspected to be  $\text{M}_6\text{C}$  type enriched with Mo.<sup>[16]</sup> They got coarsened at 800 °C (Figure 5d) and were confirmed as  $\text{M}_6\text{C}$  carbide by XRD in Figure 2b. In DED-fabricated V4E,  $\text{M}_2\text{C}$  carbides, which were identified in our previous research,<sup>[14]</sup> were observed in the as-tempered condition (Figure 5e). These precipitates were

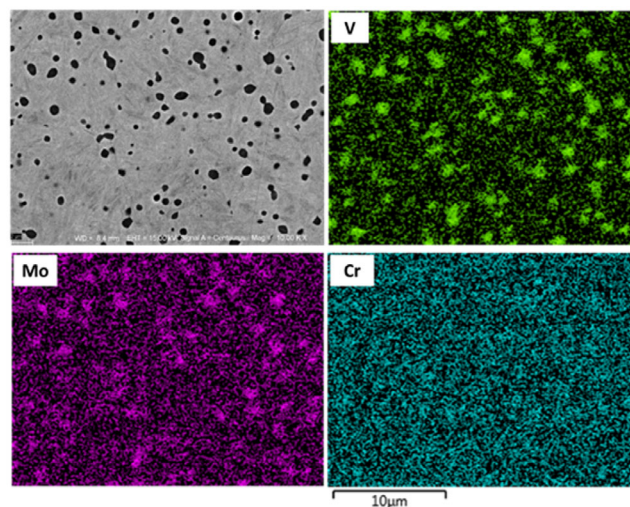


**Figure 6.** The EDS mapping results for conventional V4E in tempered condition.

mainly located close to the interdendritic zone. This can be explained by the microsegregation during the solidification process. It is generally believed that the matrix adjacent to or in the interdendritic zone has a composition distinct from the central region of the dendrite when the material is solidified at a high cooling rate. The interdendritic zone with a lower melting point contained more alloying elements including Mo. The consequence was the formation of whitish  $\text{M}_2\text{C}$  carbide enriched in Mo. However, DED-fabricated V4E steel softened at 800 °C showed a lower proportion of carbide  $\text{M}_6\text{C}$  compared to that of conventional V4E, as presented in Figure 5d,h. As mentioned in the section “Experimental Section”, the conventional V4E had already experienced a high temperature austenitizing at 1150 °C, at which the Mo-enriched carbide would be dissolved into the matrix. At high softening temperatures,  $\text{M}_6\text{C}$  carbide enriched in Mo was then precipitated, shown as the white particles in Figure 5c,d. For the DED-fabricated V4E, primary  $\text{M}_2\text{C}$  carbide formed during the solidification consumed partly Mo in the alloy, leading to a lower fraction of  $\text{M}_6\text{C}$  carbide after heating at 800 °C

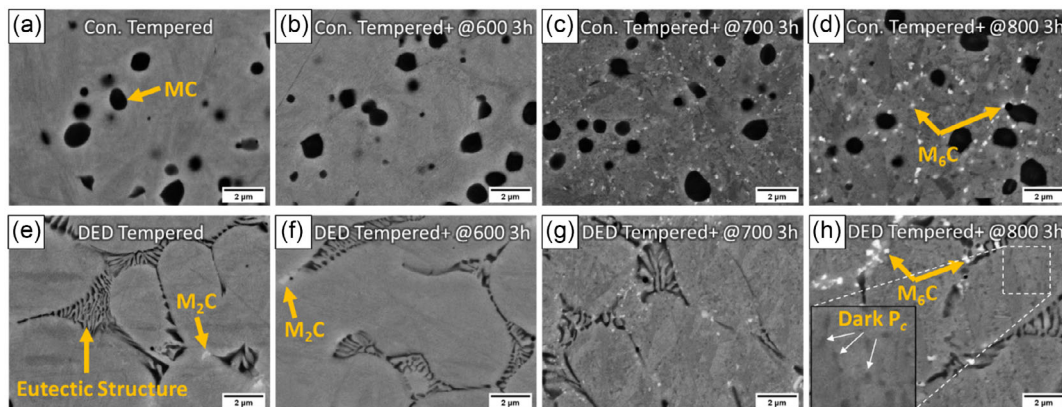


**Figure 5.** a–d) BSE images of conventional and e–h) DED-fabricated V4E after being softened at different temperatures for 3 h: a,e) as-tempered, b,f) 600 °C, c,g) 700 °C, and d,h) 800 °C.

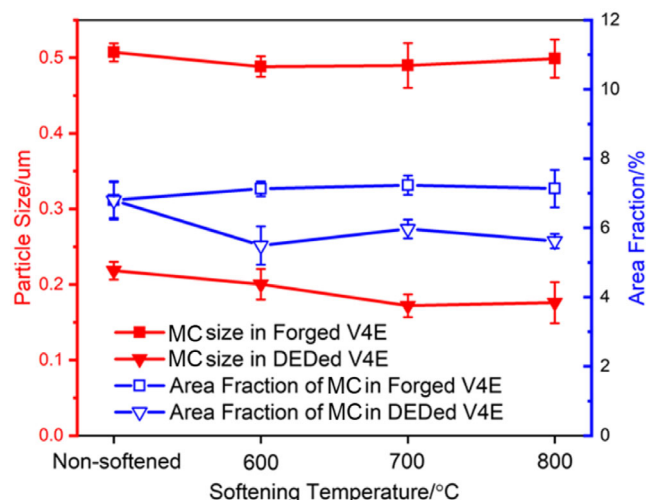


**Figure 7.** The evolution of the average size and area fraction of the MC particle in V4E after softening at 600–800 °C.

for 3 h than that for conventional V4E. In addition, some dark precipitates were also found after heating at this temperature for the softened samples, as marked by  $P_c$  and the thin arrow in the insert of Figure 5h. Considering the dark color, these precipitates should be the V-enriched MC carbide.

**Figure 8** shows the microstructures of NMS steel under different conditions. The round black features found in both conventional and DED-fabricated samples were probably porosity defects. Unlike the two previous alloys, primary carbide was seldom observed in this alloy. The microstructure of conventional and DED-fabricated samples was similar, except that some bright primary carbides (marked by orange arrows) can be seen in the HIP-fabricated samples in the tempered state (Figure 8a). These carbides were probably formed during the HIP process. The extremely low carbon content ( $\approx 0.03$  wt%) in NMS limits the carbide formation only at grain boundaries. According to our previous study,<sup>[17]</sup> extremely fine precipitates, coherent (Fe, Cr)<sub>2</sub>Mo Laves phase, are supposed to be formed during tempering. This can strongly strengthen the steel due to its fine and uniform distribution, as well as its coherency. With the magnification

used in Figure 8, the precipitates of this phase were not possible to be resolved. After softening at 600 °C, no change was observed in both conventional and DED-fabricated samples (Figure 8b,f). With increasing softening temperature, some precipitates were found in the matrix of both conventional and DED-fabricated samples (Figure 8c,d,g,h). They were believed to be the coarsened (Fe, Cr)<sub>2</sub>Mo Laves phase. No carbon was verified in these particles by EDS, which meant that they should be Laves phase instead of carbides. Some abnormally grown particles were also found in the matrix. This type of coarsening occurred first at the grain boundaries (Figure 8c,g) caused probably by the quick diffusion of alloying elements there. This result does not agree with the study by Tian et al.<sup>[18]</sup>

From the above observation, it was found that the precipitate evolution at elevated temperatures in tempered DED-fabricated and conventional samples was similar for the three alloys studied. The precipitates started to be observed after heating at the temperature of 700 °C and were then coarsened at 800 °C. The size and proportion of primary carbides/borides (for HBS and V4E, respectively), however, were stable during the softening process.

### 3.2. Softening Resistance

Hardness is a critical factor for wear resistance. As shown in **Figure 9**, the overall ranking of the hardness in the tempered and softened conditions is HBS > V4E > NMS. However, the hardness of NMS is higher than that of V4E at temperatures above 640–700 °C. All three materials showed an expected decrease in hardness with the increase in softening temperatures. The hardness of DED-fabricated steels was always higher than those of conventional counterparts under all conditions except NMS.

The softening resistance in this article is defined as the hardness drop with respect to the as-tempered condition. Compared to the HIP-fabricated counterpart, the DED-fabricated HBS presented better softening resistance. Only a slight decrease in hardness was found for 600 °C, while the hardness drop of HIP-fabricated HBS was much larger at this temperature. Notice the hardness dropped quickly for both HIP- and DED-fabricated HBS at 700 °C, indicating that this steel cannot stand

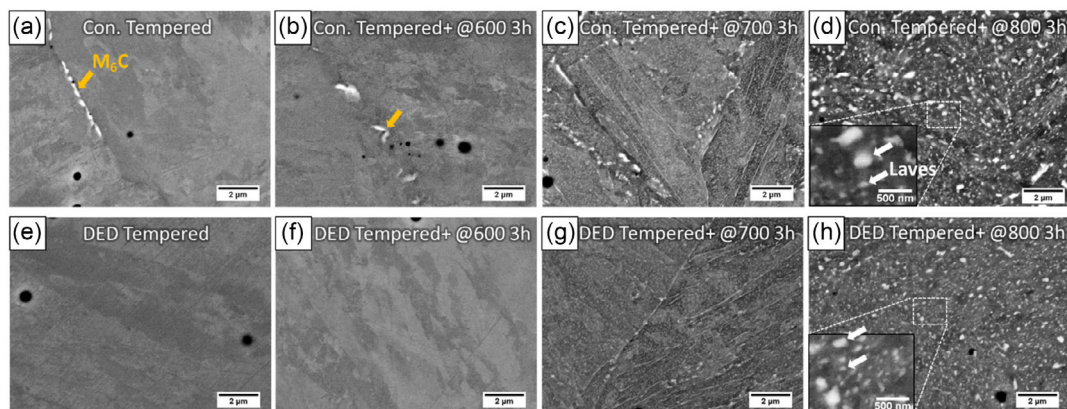


**Figure 8.** a–d) BSE images of conventional and e–h) DED-fabricated NMS after being softened at different temperatures for 3 h: a,e) as-tempered without softening, b,f) 600 °C, c,g) 700 °C, d,h) 800 °C. Carbides are marked by the orange arrows, and Laves particles are marked by the white arrows.



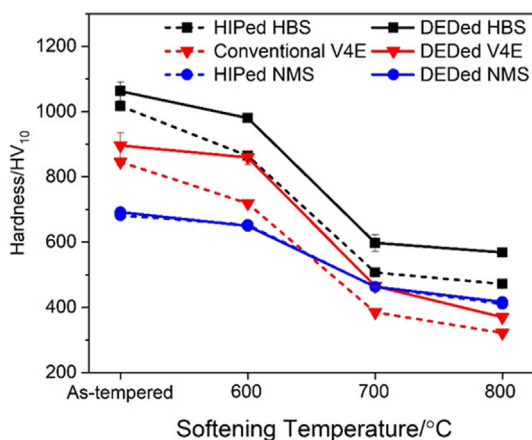


**Figure 9.** Hardness evolution of the three types of steel before and after being softened at different temperatures.

this temperature. The hardness tends to be stable at 800 °C compared to that at 700 °C.

V4E steel showed the same tendency during the softening except that it had a lower overall hardness than that of HBS (Figure 9). The hardness of this steel also had a big drop at 700 °C for both manufacturing methods.

The third type of steel, NMS, exhibited some unique characteristics. First, it presented a much less hardness decline compared to the other 2 alloys (Figure 9). With respect to the as-tempered condition, NMS had a hardness drop of  $\approx 270$  HV after being softened at 800 °C. The corresponding values for DED-fabricated HBS and V4E were about 490 and 527 HV respectively, which were much higher than that of NMS steel. This meant that NMS had outstanding softening resistance. Second, no distinct hardness difference was observed between HIP- and DED-fabricated NMS during the softening process. This could be explained by the similar microstructures observed for these two conditions (Figure 8) although a few primary carbide particles were found in the tempered state of HIP-fabricated NMS. Also, this implied that these primary carbide particles in NMS had no significant influence on its strength (based on the hardness value).

### 3.3. Abrasive Wear Resistance

Due to the target application of hot stamping, wear resistance is of great importance. In the present study, the abrasive wear test was carried out at room temperature after high-temperature exposure, and the weight reduction values were used to evaluate their abrasive wear resistance.

As shown in **Figure 10**, NMS steel had the largest weight reduction of  $\approx 250$  mg min<sup>-1</sup> among the three types of steels, indicating a comparatively poor abrasive wear resistance. However, the influence of temperature on weight reduction was insignificant. In addition, there was basically no difference between the HIP- and DED-fabricated samples in terms of weight reduction. These results echoed the similar microstructure evolution (Figure 8) and softening behavior (Figure 9) of HIP- and DED-fabricated NMS.

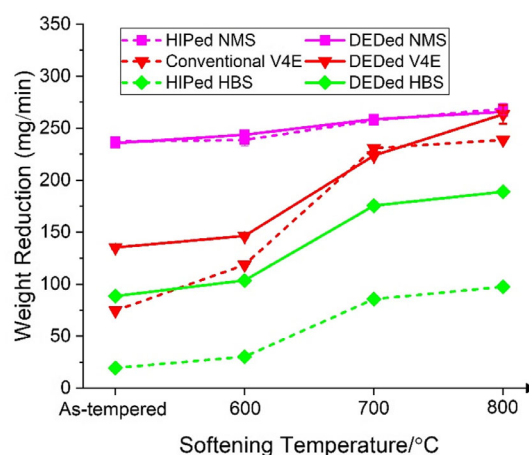


**Figure 10.** Weight reduction of the three types of steels before and after being softened at different temperatures.

The V4E steel presented a lower overall weight reduction than that of NMS steel (Figure 10), especially in the as-tempered condition, which was about 75 and 135 mg min<sup>-1</sup> for conventional and DED-fabricated samples, respectively. The weight reductions were increased with the softening temperature. For the DED-fabricated V4E steel softened at 800 °C, its weight reduction reached 260 mg min<sup>-1</sup>, which was similar to that of NMS. The weight reduction curves indicated that the abrasive wear resistance of V4E steel deteriorated quickly at temperatures of above  $\approx 700$  °C. Compared to the DED-fabricated counterpart, the weight reductions of conventional V4E samples were lower except for the condition at 700 °C. This meant that the conventional V4E steel in general had a better abrasive wear resistance than the DED-fabricated counterpart.

This phenomenon was further magnified for the HBS steel. As can be seen in Figure 10, the HIP-fabricated HBS samples had extremely low weight reductions. The large difference in weight reduction between conventional and DED-fabricated HBS indicated that DED-fabricated counterpart had much worse wear resistance. The reason will be discussed in Section 4.2. In addition, both HBS and V4E showed a sharp increase in weight reduction for softening at 700 °C, which was consistent with the microstructure evolution and the softening tendency in terms of hardness.

For the as-worn surface topographies, as revealed in **Figure 11**, the grooves on the HIP-fabricated HBS were shallower (Figure 11a–d) and less than those on DED-fabricated samples (Figure 11e–h). In Figure 11a–d, it was found that even the boride particles could be ploughed to some extent in the HIP-processed HBS. This meant the hard asperities, i.e., Al<sub>2</sub>O<sub>3</sub>, had comparable hardness with the boride, which agreed with the literature. In ref. [19], the reported hardness of Al<sub>2</sub>O<sub>3</sub> phase is  $\approx 2000$  HV, while the M<sub>3</sub>B<sub>2</sub> boride (the primary hard phase in HBS) has a hardness of between 1600 to 2400 HV.<sup>[20]</sup> When the hard asperities (Al<sub>2</sub>O<sub>3</sub> particle in the present study) met the boride particles, the groove tracks were much shallower than that in the matrix, implying that borides contributed greatly to the abrasive wear resistance. With the increase in softening temperature, the grooves in HIP-processed HBS become deeper and



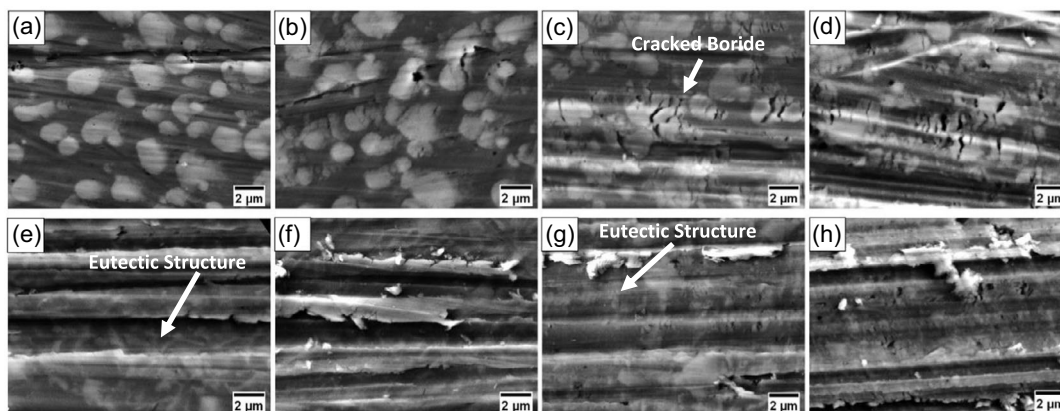


**Figure 11.** a–d) The worn surface of conventional and e–h) DED-fabricated HBS after being softened at different temperatures for 3 h: a,e) as-tempered, b,f) 600 °C, c,g) 700 °C, and d,h) 800 °C.

deeper and their number increased as well. Another interesting phenomenon observed for HIP-processed HBS was the extensive cracking of borides at high softening temperatures (Figure 11c, d). Although some cracked borides had already been found in the softened samples (Figure 1c,d), the number of cracks was significantly less than that in the wear-tested samples. It meant crack propagation in boride particles, or more boride particles were broken during the wear test. However, as can be seen in Figure 11c,d, the cracked boride particles still had a strong resistance against deformation and provided wear resistance in the steel.

The cracked boride particles were hardly seen in DED-fabricated HBS samples attributed to the smaller average particle size. In addition, there was some fatigue debris along the edge of grooves in the high-temperature softened DED-fabricated sample (Figure 11f–h). These debris particles were formed as the result of fatigue by repeated ploughing and contributed to weight reduction. These observations were consistent with the data presented in Figure 10.

For V4E steel, the as-tempered conventional V4E sample (Figure 12a) revealed a distinct small penetration depth of wear tracks compared to the softened samples (Figure 12b–d). The

coarse MC particles could be clearly seen and stayed intact. With the increase in softening temperature, the edge of the grooves became rougher (Figure 12c,d). However, the situation was different in DED-fabricated V4E. The grooves became deep already in the as-tempered condition and were similar in the softened conditions. A similar tendency was observed in DED-fabricated HBS as well. The worn surfaces of NMS samples showed very rough surface topography and were similar for all conditions (Figure 13).

## 4. Discussion

### 4.1. The Softening Resistance

As shown in Figure 9, the HIP-processed HBS has a bigger hardness drop than the DED ones, indicating that DED-fabricated HBS has a superior softening resistance to the HIP-fabricated counterparts. The reason for this could be explained by the fast cooling rate in additive manufacturing, which will lead to more alloying elements trapped in the matrix during the solidification. At elevated temperatures, some alloying elements could then combine with carbon and form fine carbide to strengthen the

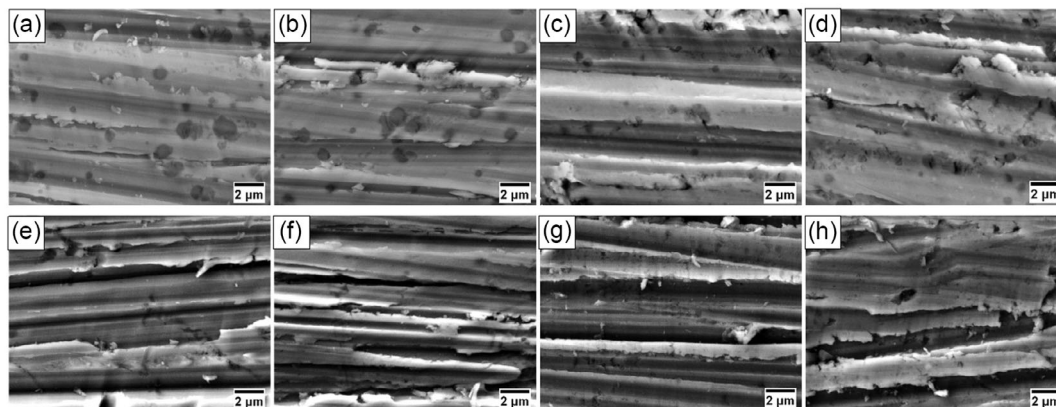


**Figure 12.** a–d) The worn surface of conventional and e–h) DED-fabricated V4E after being softened at different temperatures for 3 h: a,e) as-tempered, b,f) 600 °C, c,g) 700 °C, and d,h) 800 °C.

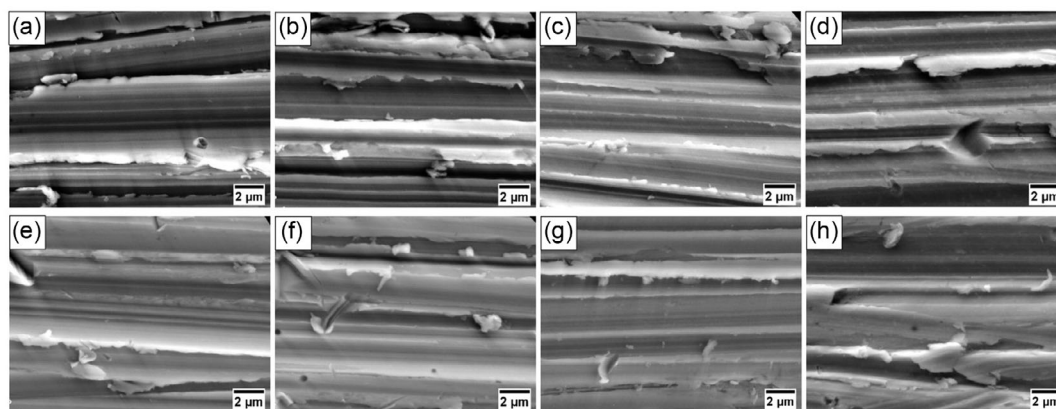


**Figure 13.** a–d) The worn surface of conventional and e–h) DED-fabricated NMS after being softened at different temperatures for 3 h: a,e) as-tempered, b,f) 600 °C, c,g) 700 °C, and d,h) 800 °C.

matrix, providing a kind of secondary hardening effect. As can be seen in Figure 1d,h, more fine particles are found in the DED-fabricated HBS after softening at 800 °C, providing a higher precipitation-strengthening effect and consequently better softening resistance.

For V4E steel at 600 °C, compared to the as-tempered condition, the DED-fabricated sample also has a smaller hardness drop, i.e., better softening resistance than the forged one. The reason for this is that the tempered conventional V4E steel is supposed to have a higher dislocation density than the DED-fabricated counterpart due to the lower tempering temperature used (525 °C). When subjected to softening at 600 °C, the forged V4E will experience quick annihilation of dislocations, leading to a bigger drop in the hardness. The dislocation density in forged V4E steel will then be similar to forged and DED-fabricated V4E samples, leading also to similar softening resistances at the higher softening temperatures of 700 and 800 °C. However, the DED-fabricated V4E has an overall initial higher hardness than the forged variant (Figure 9). This can be explained by the different extent of the precipitate hardening effect. As shown in Figure 5, the dark precipitates in the matrix are V-enriched MC carbide. The proportion of MC primary carbide (the coarse type) in DED-fabricated V4E (5.5%) is lower than that in forged ones (7.1%), as indicated by the area fraction in Figure 7. This means that more V is trapped in solid solution in the matrix of DED-fabricated V4E. Consequently, more V-enriched fine MC carbides (marked by Pc and the thin arrow in the insert of Figure 5h) will be formed in the subsequent tempering and softening treatments, contributing to a stronger precipitation strengthening effect than that in conventional V4E.

The NMS steel is a maraging steel with extremely low carbon content. Basically, the major strengthening mechanism in maraging steel is precipitation hardening with intermetallic compound particles. In our previous study, the influence of precipitation on the softening behavior of NMS steel has been studied.<sup>[17]</sup> Stable C14-Laves phase particles are considered as the major reinforcing phase. The superior softening resistance is attributed to the low coarsening rate of Laves phase originated from the low diffusion coefficient of the controlling element (Mo) and low interfacial energy with the surrounding matrix.

Compared to the as-tempered state, the hardness drop is around 270 HV for 800 °C and 150 HV for 600 °C.<sup>[17]</sup> This difference can be explained by the diffusivity of the controlling element (Mo) at these two temperatures. It is about 4 orders of magnitude higher at 800 °C than that at 600 °C. However, the hardness difference between HIP- and DED-fabricated NMS is ignorable due to similar microstructures in both as-tempered and softened conditions.

## 4.2. The Wear Mechanism

The abrasive wear resistance of steels usually depends on several factors, such as the hardness of the material, the proportion, shape, size, and distribution of reinforcing secondary phase precipitates, as well as the general strength of the matrix.<sup>[1]</sup> As described in Section 3.2, the abrasive wear in this study is presented as microploughing. Attempts have been made in this section to interpret the abrasive wear resistance of the studied steels.

Hardness is a critical factor for wear resistance. The ranking of the overall wear resistance at room temperature for three types of steels in the tempered and softened condition is HBS > V4E > NMS. The hardness ranking basically follows the same sequence until ≈640–700 °C. However, the hardness of as tempered NMS is significantly higher than that of softened conventional V4E at 800 °C (Figure 9), while the corresponding wear resistance is the opposite (Figure 10). This means hardness is not the only factor that affects the wear resistance.

As shown in Figure 10, the HIP-processed HBS steel shows a distinct higher abrasive wear resistance than DED-fabricated HBS. In contrast, the hardness of HIP-fabricated HBS is lower than DED-fabricated counterpart in all conditions (Figure 9). This confirms again that hardness alone cannot explain the high wear resistance of the HIP-fabricated HBS. As can be seen in Figure 1, the reinforcing phase particles, which are the coarse and round particles of  $M_3B_2$  boride, are evenly distributed in the matrix in HIP-fabricated HBS samples. However, for DED-fabricated HBS, the boride phase is nonuniform with either square or eutectic morphology. There also exists boride-free zone. Despite an almost equal proportion as in the DED-fabricated sample, the boride in HIP-fabricated HBS possesses a much higher

particle mean size (typically 3 times higher), as shown in Figure 4. A hypothesis hence can be proposed. For given steel grade, large and uniformly distributed hard particles are beneficial to the abrasive wear resistance, the effect of which is related to the ratio of particle spacing ( $\lambda$ ) and average width ( $d_g$ ) of the grooves.

Free spacing  $\lambda$  between two reinforcing particles can be used to evaluate the abrasive wear resistance to a certain extent (Keränen, 2010). It can be written as Equation (1)<sup>[21,22]</sup>

$$\lambda = \frac{d_p}{2} \left( \sqrt{\frac{2\pi}{3f_v}} - 1 \right) \quad (1)$$

where  $d_p$  is the average diameter of particles, and  $f_v$  is the volume fraction of the reinforcing phase. When the ratio  $\lambda/d_g > 1$  ( $d_g$  is the average width of grooves), the hard asperities from the erodent material may scratch the matrix and plough away the matrix material easily, leading to a reduction of the wear resistance. For the ratio  $\lambda/d_g < 1$ , on the contrary, the hard asperities cannot easily embed into the matrix and plough the materials, implying increased wear resistance. This is because the hard asperities will scratch the reinforcing particles instead of the matrix when  $\lambda$  is smaller than the sizes of the hard asperities. For HIP-fabricated HBS, the estimated  $\lambda$  from Equation (1) is about  $\approx 1.2 \mu\text{m}$ . From the images of worn surfaces in Figure 11, the  $d_g$  is estimated to be about  $\approx 1.5 \mu\text{m}$ , which is larger than  $\lambda$ . Therefore,  $\lambda/d_g < 1$ , meaning the HIP variant of HBS has outstanding abrasive wear resistance. The schematic diagram for HIP-fabricated HBS steel is shown in Figure 14a). For DED-fabricated HBS, the situation is different due to the existence of eutectic structure which is relatively finer (Figure 1). The regions with the eutectic structure would have a lower hardness compared to the pure  $\text{M}_3\text{B}_2$  boride in conventional samples. Hence, as can be seen in Figure 11, these regions are easy to be broken and pulled up when facing the ploughing of hard asperities ( $\text{Al}_2\text{O}_3$  particle with a hardness of  $\approx 2000 \text{ HV}$ ). Moreover, the coarse boride particles with a square shape have a much lower volume fraction, which will result in a much larger  $\lambda$ . In this case, the matrix material can be easily ploughed away, resulting in low wear resistance. In addition, the material in the boride-free regions is also easy to be scratched away, which deteriorates further the wear resistance of DED-fabricated HBS steel.

The situation for V4E steel is similar to that of HBS. Conventional V4E steel has coarse and uniformly distributed MC carbide particles (Figure 5) and hence shows better wear

resistance than the DED-fabricated V4E material. The  $\lambda$  value of primary MC carbides in conventional V4E is about  $1.7 \mu\text{m}$ , which is slightly larger, but still close to the  $d_g$  ( $\approx 1.5 \mu\text{m}$ ). As a result, the as-tempered conventional V4E sample shows decent wear resistance but still is not as good as that of the HIP-fabricated HBS, as schematically shown in Figure 14b). Similar to HBS, as-tempered DED-fabricated V4E shows a worse wear resistance despite of high hardness. This is because instead of a round coarse shape, the reinforcing MC carbide now is present in a eutectic form, which cannot stand the scratch from hard asperities.

As can be seen in Figure 10, NMS shows the worst overall abrasive wear resistance among the three studied grades of steel. Even if the matrix is strengthened by nanoprecipitates (C14-Laves phase), the hard  $\text{Al}_2\text{O}_3$  asperities, which have an extremely high hardness, can still remove the matrix materials easily owing to the absence of coarse hard particles, as shown in Figure 14c). Although NMS has a hardness higher than that of conventional V4E at 700 and 800 °C (Figure 9), the weight reductions of NMS during wear tests are higher than conventional V4E samples (Figure 10). The reduced wear resistance is due to that the conventional V4E steel has the coarse hard particles, which can stop the further wear until the entire particles are pushed away. The narrow free spacing  $\lambda$  between primary hard particles is of great importance for good wear resistance. Another possible factor affecting wear resistance is the hardness of the reinforced particles. The hardness of the reinforced phase, i.e., the C14-Laves phase, in NMS is about  $\approx 1460 \text{ HV}$ ,<sup>[23]</sup> which is lower than the  $\text{M}_3\text{B}_2$  and MC in the other two steels. This could be another reason for the low wear resistance of NMS. Further investigation is needed.

For all three investigated steels, in general, the samples softened at higher temperatures have more weight reduction. Still, from the microstructure observation, the volume fraction of the primary reinforcing phases (the  $\text{M}_3\text{B}_2$  boride in HBS and the MC carbide in V4E) did not change that much. Therefore, the softening of surroundings (precipitates coarsening, decreasing of dislocation density, and so on) in HBS and V4E is suspected to be the reason for the deterioration of the abrasive wear resistance at high temperatures. The softened surroundings provide low resistance against plastic deformation and therefore can be ploughed away easily. It can be seen in Figure 11 and 12 that with the increase of softening temperature, the edge of groove tracks becomes rougher. When subjected to the force from hard  $\text{Al}_2\text{O}_3$

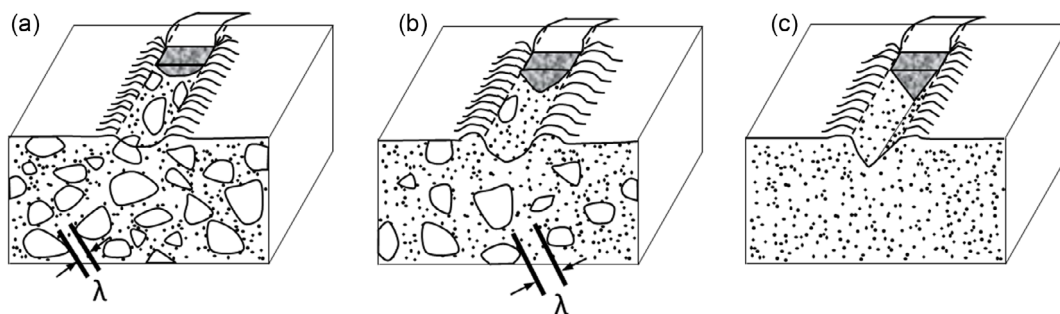


**Figure 14.** Schematic diagram of wear mechanisms in the three conventional steels: a) HBS with small free spacing  $\lambda$ , b) V4E with large free spacing  $\lambda$  among particles, and c) NMS. The small dots represent fine hard-phase particles in the matrix. The big particles represent the coarse hard-phase particles.



asperities, the softened material surrounding the primary reinforcing phases was pushed away to both sides of the groove. With repeated deformation under the action of the hard asperities, some fatigue debris is formed on the groove's edges. These rough edges may eventually peel off, resulting in a significant material loss. The excellent softening resistance of NMS makes the wear resistance of this steel only varies slightly with temperature.

## 5. Conclusion

Three types of tool steels were cladded on a hot work tool steel by means of DED. The softening resistance and wear resistance have been investigated systematically on the cladded materials and compared with their conventional counterparts. The correlation between these properties and microstructure was clarified. The key conclusions are presented as follows: 1) The microstructure of DED-fabricated HBS differs significantly from that of conventional ones. Relatively large round primary boride in the form of  $M_3B_2$  is found in conventional steel in both as-tempered and softened conditions. The size ( $\approx 1.2\text{--}1.3\text{ }\mu\text{m}$ ) and the fraction ( $\approx 0.21$ ) of this phase are almost constant in these conditions. Besides a few primary boride in a square shape, eutectic structures and boride-free regions are also found in AM-produced counterparts. The average size of the boride is reduced significantly to  $\approx 0.4\text{ }\mu\text{m}$  and maintained almost constant in all conditions. At temperatures at and above  $700\text{ }^\circ\text{C}$ , precipitates in the form of  $M_{23}C_6$  and  $M_6C$  are observed in both AM and conventional HBS. These precipitates become coarser at the higher temperature of  $800\text{ }^\circ\text{C}$ . Compared to conventional HBS, there are more precipitates in DED-fabricated samples because more alloying elements are trapped in the matrix due to the fast solidification; 2) The microstructure of DED-fabricated V4E also differs significantly from that of conventional ones in both as-tempered and softened conditions. Primary round MC carbide is observed in conventional V4E. In the DED-fabricated counterpart, MC exists in the form of a eutectic structure and  $M_2C$  carbide is formed as well. The fraction and size of MC carbides are rather stable during the softening process for both AM and conventional V4E. However, MC carbide in DED-fabricated V4E is smaller ( $\approx 0.2\text{ }\mu\text{m}$ ) and less (5.5%) than that in its conventional counterpart ( $\approx 0.5\text{ }\mu\text{m}$  and 7.1%). At temperatures above  $700\text{ }^\circ\text{C}$ ,  $M_6C$  carbide is observed and gets coarser at the higher temperature of  $800\text{ }^\circ\text{C}$ . Compared to conventional V4E, less  $M_6C$  carbide is formed in DED-fabricated V4E, but some fine carbide (possibly V-enriched MC) can be precipitated at this temperature; 3) Unlike HBS and V4E, the microstructure of conventional and DED-fabricated NMS samples is similar in both as-tempered and softened conditions. Primary carbide is seldom observed. The major strengthening phase in this steel is the coherent C14-Laves phase  $((Fe, Cr)_2Mo)$  which is fine and uniformly distributed after tempering. With the increase in softening temperature, this phase is coarsened slowly; 4) All three materials show a decreased hardness with the increase in softening temperatures. There is a significant hardness drop when the softening temperature reaches  $700\text{ }^\circ\text{C}$  for HBS and V4E. Compared to their conventional counterparts, DED-fabricated HBS and V4E possess higher hardness and better softening resistance, defined

as the hardness drop with respect to the as-tempered condition. This can be explained by the fast solidification in the DED process. More alloying elements are trapped in the matrix, leading to an increased number of certain precipitates (possibly  $M_{23}C_6$  for HBS and MC for V4E) that can provide a hardening effect; 5) The investigated NMS has the lowest initial hardness in the tempered state but the best softening resistance. This is owing to the fine C14-Laves precipitate which is thermodynamically stable and coherent with a small lattice mismatch. The consequent slow coarsening makes its hardness higher than that of V4E at temperatures above  $\approx 640\text{--}700\text{ }^\circ\text{C}$ . In addition, there is no difference in hardness between DED samples and conventional counterparts under all conditions due to similar microstructure; 6) The ranking of the overall wear resistance at room temperature for three types of steels in the tempered and softened condition is  $HBS > V4E > NMS$ . Overall, the hardness ranking follows the same sequence, indicating hardness is one of the important factors that determines wear resistance. The samples exposed at higher temperatures have more weight reduction for all three investigated steels. For HBS and V4E, the quick deterioration of the abrasive wear resistance at  $700\text{ }^\circ\text{C}$  and above is due to the softening of the matrix surrounding the primary reinforcing phases caused by precipitates coarsening, a decrease of dislocation density, and so on. Compared to HBS and V4E, the influence of temperature on the weight reduction of NMS is less significant, attributed to its excellent softening resistance; 7) Conventional HBS and V4E have better wear resistance compared with DED-fabricated counterparts despite lower hardness. There exists a large difference in weight reduction between conventional and DED-fabricated HBS. The free spacing  $\lambda$  between hard coarse particles is another important factor that influences the wear resistance. A small  $\lambda$  (strictly speaking, a small ratio of  $\lambda/d_p$ ) contributes to superior wear resistance. Less/absence of coarse hard particles and the existence of weak eutectic structure explains why DED-fabricated HBS and V4E have worse wear resistance than the conventional ones; and 8) Among the three steels investigated, NMS has the worst abrasive wear resistance at RT for both DED-fabricated and conventional samples. The absence of big primary hard particles and the relatively soft and fine C14-Laves phase (major strengthening phase in this steel) in the matrix are supposed to be the major reasons. Due to similar microstructure, no difference in wear resistance is observed between DED-fabricated NMS and conventional counterparts under all conditions.

## Acknowledgements

This study is supported by Production Area of Advance, Chalmers University of Technology, China Scholarship Council (grant no. 201806370253), Uddeholms AB, Sweden, and ASSAB Tooling Technology, China.

## Conflict of Interest

The authors declare no conflict of interest.

## Data Availability Statement

The data that support the findings of this study are available from the corresponding author upon reasonable request.

## Keywords

directed energy deposition, softening resistances, tool steel, wear resistance

Received: August 29, 2023

Revised: March 12, 2024

Published online:

- [1] S. H. Wang, J. Y. Chen, L. Xue, *Surf. Coat. Technol.* **2006**, 200, 3446.
- [2] B. D. Beake, L. Ning, C. Gey, S. C. Veldhuis, A. B. Kornberg, A. Weaver, M. Khanna, G. S. Fox-Rabinovich, *Surf. Coat. Technol.* **2015**, 279, 118.
- [3] M. Pellizzari, *Wear* **2011**, 271, 2089.
- [4] A. Persson, S. Hogmark, J. Bergström, *Surf. Coat. Technol.* **2005**, 191 216.
- [5] S. Pant, S. Kumar, A. S. Shahi, *Mater. Today: Proc.* **2023**.
- [6] S. I. Evans, J. Wang, J. Qin, Y. He, P. Shepherd, J. Ding, *Structures* **2022**, 44, 1506.
- [7] P. Kattire, S. Paul, R. Singh, W. Yan, *J. Manuf. Process.* **2015**, 20, 492.
- [8] J. Leunda, C. Soriano, C. Sanz, V. G. Navas, *Phys. Proc.* **2011**, 12, 345.
- [9] J. Nurminen, J. Näkki, P. Vuoristo, *Int. J. Refract. Hard Met.* **2009**, 27, 472.
- [10] M. Orečný, M. Buršák, M. Šebek, L. Falat, *Metals* **2016**, 6, 236.
- [11] R. Colaco, R. Vilar, *Wear* **2005**, 258, 225.
- [12] R. Colaco, C. Pina, R. Vilar, *Scr. Mater.* **1999**, 41, 715.
- [13] N. U. Rahman, M. B. De Rooij, D. T. A. Matthews, G. Walmag, M. Sinnaeve, G. R. B. E. Römer, *Tribol. Int.* **2019**, 130, 52.
- [14] M. Yuan, S. Karamchedu, Y. Fan, L. Liu, L. Nyborg, Y. Cao, *J. Manuf. Process.* **2022**, 76, 419.
- [15] S. H. Chang, C. Y. Chuang, K. T. Huang, *ISIJ Int.* **2019**, 59, 1354.
- [16] C. Botero, M. Ramsperger, A. Selte, K. Åsvik, A. Koptug, P. Skoglund, S. Roos, L. E. Rännar, M. Bäckström, *Steel Res. Int.* **2020**, 91, 1900448.
- [17] M. Yuan, L. Nyborg, C. Oikonomou, Y. Fan, L. Liu, Y. Cao, *Mater. Des.* **2022**, 224, 111393.
- [18] Y. Tian, K. Chadha, S. H. Kim, C. Aranas, *Mater. Sci. Eng. A* **2021**, 805, 140801.
- [19] C. Piconi, in *Comprehensive Biomaterials II*, Elsevier, Oxford **2017**.
- [20] Y. Tomota, K. Kuroki, T. Mori, I. Tamura, *Mater. Sci. Eng.* **1976**, 24, 85.
- [21] K. Li, L. Wei, B. An, B. Yu, R. D. K. Misra, *Mater. Sci. Eng. A* **2019**, 739, 445.
- [22] M. Keränen, Ph.D. Thesis, Aalto University, Finland **2010**.
- [23] W. Luo, C. Kirchlechner, J. Li, G. Dehm, F. Stein, *J. Mater. Res.* **2020**, 35, 185.